

Stratified Turbulent-Turbulent Gas-Liquid Flow in Horizontal and Inclined Pipes

A two-dimensional model for stratified turbulent-turbulent gas-liquid flow in inclined pipes is proposed. The gas phase is treated as bulk flow, but an exact solution is carried out for the liquid phase, applying the eddy viscosity theory to model the turbulent viscosity. The interfacial structure is taken into consideration using appropriate correlations for the interfacial shear stress. The model is capable of predicting the liquid velocity field, holdup and pressure drop given gas and liquid flow rates, physical properties, pipe size, and angle of inclination. The results are substantially better than the prediction of Lockhart and Martinelli (1949) correlation and better than the Taitel and Dukler (1976) model for stratified flow.

OVADIA SHOHAM and
YEHUDA TAITEL

Faculty of Engineering
Tel-Aviv University
Tel-Aviv, Israel 69978

SCOPE

Stratified flow can exist in horizontal flow as well as in downward and upward inclined flow. In downward inclinations stratified flow is the dominant flow regime, while in upward flow it occurs over a smaller range of flow rates, depending on the inclination angle. As the angle of inclination increases, the region of stratified flow decreases and finally completely disappears. It does, however, usually exist at the entrance region in slug flow, which is the dominant flow regime in the upward configuration.

Although stratified gas-liquid flow occurs in horizontal as well as in inclined pipes, consideration over the past 25 years has been given mainly to the horizontal configuration. Also the

analyses were restricted either to laminar flow or, for turbulent flow, a simplified, usually one-dimensional approach, was used.

It is the purpose of this study to develop a two-dimensional model for stratified turbulent liquid and laminar or turbulent gas flow in horizontal and inclined pipes in order to predict the two-dimensional liquid velocity field, pressure drop and holdup. This is achieved by applying an exact solution of the Navier Stokes equation of motion for the liquid-phase utilizing the eddy viscosity concept. The results are tested against experimental data available in the literature.

CONCLUSIONS AND SIGNIFICANCE

A procedure for the prediction of the liquid velocity field, holdup and pressure drop has been developed for stratified turbulent flow in horizontal and inclined pipes. The analysis is carried out by solving the two-dimensional equation of motion for the liquid phase. The interfacial structure is taken into consideration using appropriate correlations for the interfacial stress. The procedure incorporates eddy viscosity theory for the turbulent viscosity.

The predicted liquid velocity field in upward inclined flow is completely different from that in horizontal flow, as backward flow may occur near the bottom pipe wall. Predicted pressure drop and holdup are tested against available experimental data in the literature, showing substantially better agreement than the predictions of Lockhart and Martinelli (1949) correlation, Taitel and Dukler (1976), and others.

INTRODUCTION

A solution for turbulent stratified pipe flow is quite complex due to: 1. the two dimensionality of the flow field and 2. the uncertainty of the interfacial shear. As a result, the approaches taken in the past were considerably simplified using generally either empirical correlations or a one-dimensional approach.

One of the first and most durable empirical correlation for pressure drop and holdup in horizontal flow was proposed by Lockhart and Martinelli (1949). Although the partially physical interpretation of the correlation is that of a separated flow structure, it was based on experimental data spanning various other flow patterns, such as slug and annular flows. This is the main reason for errors of more 100% reported on the application of the correlation in stratified flow. An extension of this model was done by Johannessen (1972) who evolved a theoretical model which agrees better than Lockhart and Martinelli's correlation with the experimental results.

Mechanistic approaches have been used to predict turbulent stratified flow parameters in horizontal flow. Etchells (1970), Govier and Aziz (1972), Agrawal et al. (1973), and Russell et al. (1974) calculated the frictional pressure drop as in single-phase flow using a geometrical model for the flow cross-section.

Taitel and Dukler (1976) proposed a model for predicting flow regime transition in horizontal and near-horizontal gas-liquid flow. Their approach is to assume stratified conditions and then to determine the mechanism by which stratified flow changes to any other flow pattern. This approach is based on the observation that stratified flow may exist as an entry region in the pipe, also for nonstratified flow regimes. Their model for stratified flow is a one-dimensional model, since both phases are treated as bulk flow. This approach neglects the detailed velocity profile structure and the shear stresses are calculated via empirical correlations based on the average velocity. Such an approach could be in serious error for calculating the shear stresses at the bottom pipe for upward inclined flows. In the latter case the flow near the bottom of the pipe may be negative resulting in an opposite value for the shear stress compared to its value calculated on the basis of the "one-dimensional" theory.

Present address of O. Shoham: Petroleum Engineering Department, The University of Tulsa, OK 74104.

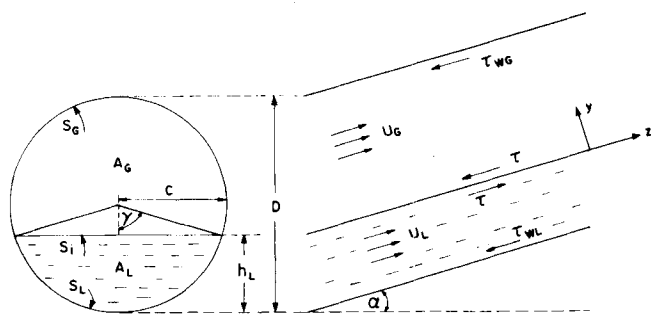


Figure 1. Stratified flow system in inclined pipes.

An extension of the model of Russell et al. (1974) to turbulent-turbulent gas-liquid stratified flow in horizontal pipes was carried out by Cheremisinoff and Davis (1979). Their analysis of the turbulent liquid phase is based on the approach of Dukler (1960), who used successfully available turbulent mixing length theory for downward annular two-phase flow. The expressions used for the eddy viscosity were Deissler's equation for the region near the wall and Von Karman's equation for the turbulent core. In order to simplify their model, Cheremisinoff and Davis assumed a constant shear stress in the whole liquid region, $\tau = \tau_w = \text{const}$, and a velocity profile which depends only on the radial position $u = u(r)$. Solving for the velocity profile under these assumptions, a universal dimensionless turbulent profile is constructed.

Though the Cheremisinoff and Davis results should apply fairly well for shallow liquid layers, $h_L/D \ll 1$, it may introduce serious errors for thick layers and inclined pipes where both assumptions of constant shear stress and the dependence of the velocity profile on the radial position only do not apply.

Recently Kadambi (1981) suggested an analytical procedure to determine the pressure drop between two parallel plates. He showed that the velocity profile of the gas and the liquid could be represented by two hypothetical fully-developed flow profiles using matching conditions at the interface. Pai polynomial velocity profile was used which is applicable over the whole range of Reynolds number so that the solution is valid for both laminar and turbulent flow. The use of the equivalent pipe diameter concept has enabled the results to be of general value for pipes as well as for flat plates and rectangular channels.

ANALYSIS

Figure 1 shows the geometry of the stratified flow considered. The liquid level in the pipe is h_L and it flows concurrently with a

gas layer above it. The pipe is upwardly inclined with an angle $+\alpha$.

Under steady-state conditions the Navier Stokes equations for each for the layers reduce to:

$$\nabla^2 u_L = \frac{1}{\mu_{eL}} \left(\frac{dP}{dz} + \rho_L g \sin \alpha \right) \quad (1)$$

$$\nabla^2 u_G = \frac{1}{\mu_{eG}} \left(\frac{dP}{dz} + \rho_G g \sin \alpha \right) \quad (1')$$

where μ_e denotes the effective viscosity, which equals the sum of the molecular viscosity and the turbulent eddy viscosity

$$\mu_e = \mu + \mu_t \quad (2)$$

The boundary conditions are:

- 1) $u_G = 0$ at the upper wall (no slip condition).
- 2) $u_L = 0$ at the lower wall (no slip condition).
- 3) $\mu_{eL} \frac{\partial u_L}{\partial y} = \tau_i$ at the interface (continuity of velocity and shear stress)
- 4) $u_L = u_G$
- 5) $\frac{\partial u_L}{\partial x} = \frac{\partial u_G}{\partial x} = 0$ at the normal midplane (symmetry)

Introducing dimensionless variables

$$u'_L = \frac{u_L}{u_{LS}} \quad u'_G = \frac{u_G}{u_{GS}} \quad y' = \frac{y}{D} \quad x' = \frac{x}{D} \quad z' = \frac{z}{D} \quad A' = \frac{A}{D^2} \quad (3)$$

$$P'_L = \frac{P}{\rho_L u_{LS}^2} \quad P'_G = \frac{P}{\rho_G u_{GS}^2} \quad \mu'_L = \frac{\mu_L}{\rho_L D u_{LS}} \quad \mu'_G = \frac{\mu_G}{\rho_G D u_{GS}}$$

the governing equations become

$$\nabla'^2 u'_L = \frac{1}{\mu'_{eL}} \left(\frac{dP'}{dz'} + \rho'_L g \sin \alpha \right)'_L = \frac{K'_L}{\mu'_{eL}} \quad (4)$$

$$\nabla'^2 u'_G = \frac{1}{\mu'_{eG}} \left(\frac{dP'}{dz'} + \rho'_G g \sin \alpha \right)'_G = \frac{K'_G}{\mu'_{eG}} \quad (4')$$

where

$$\mu'_{eL} = 1/Re_{LS} + \mu'_{iL}; \quad \mu'_{eG} = 1/Re_{GS} + \mu'_{iG} \quad (5)$$

$$Re_{LS} = \frac{u_{LS} D}{\nu_L}; \quad Re_{GS} = \frac{u_{GS} D}{\nu_G} \quad (5')$$

One of the difficulties in solving the problem is caused by the inhomogeneity of the boundaries, which consist of a circular surface (the wall) and a plane (the interface). This difficulty is alleviated by using bipolar coordinates. The bipolar coordinates are the natural coordinate system to be used in dealing with field problems whose boundaries consist of intersecting circular cylinder with a plane.

If the intersection points are $S_1(c, 0)$ and $S_2(-c, 0)$, as shown in

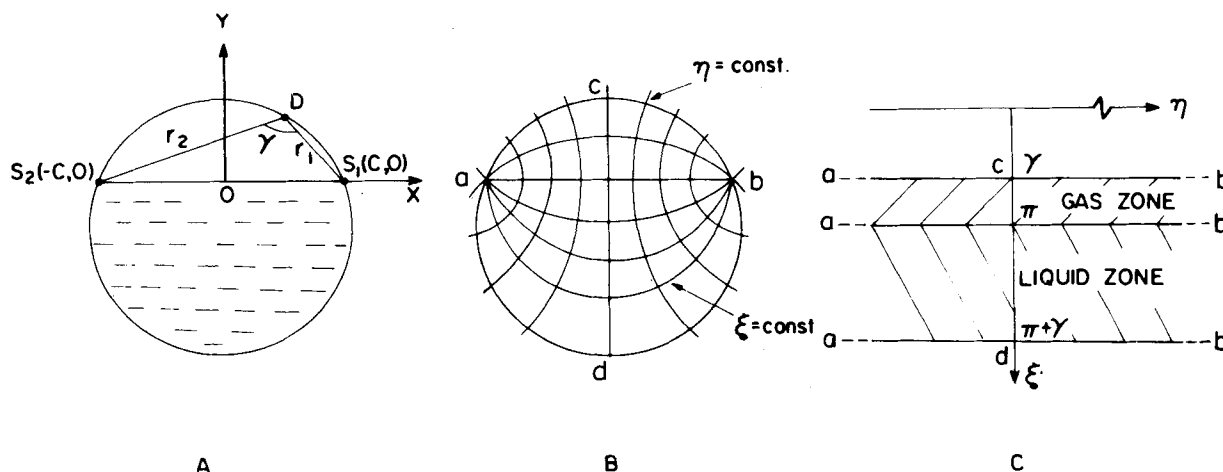


Figure 2. Bipolar coordinate system.

Figure 2A, the conformal transformation which defines the bipolar coordinates is

$$\omega = ic \cot(\zeta/2)(i = (-1)^{1/2}) \quad (6)$$

where $\omega = x + iy$, $\zeta = \xi + i\eta$ and $(x, y)/(\xi, \eta)$ are the coordinates in the ω -plane and the ζ -plane respectively. This conformal mapping allows the transformation of the gas and liquid cross sections into two infinite strips (as shown in Figure 2C)

$$\begin{aligned} \gamma < \xi < \pi & \quad -\infty < \eta < \infty & \text{for the gas} \\ \pi < \xi < \pi + \gamma & \quad -\infty < \eta < \infty & \text{for the liquid} \end{aligned}$$

Transforming the dimensionless governing equations into bipolar coordinates yields

$$\frac{\partial^2 u'_L}{\partial \xi^2} + \frac{\partial^2 u'_L}{\partial \eta^2} = \frac{K'_L}{\mu'_{eL} (\cosh \eta - \cos \xi)^2} c'^2 \quad (7)$$

$$\frac{\partial^2 u'_G}{\partial \xi^2} + \frac{\partial^2 u'_G}{\partial \eta^2} = \frac{K'_G}{\mu'_{eG} \cosh \eta - \cos \xi)^2} c'^2 \quad (7')$$

A solution for both the liquid and the gas regions can be obtained satisfying matching conditions at the interface. Such a solution will be applicable only to smooth surfaces; in addition, it will be quite complex. In principle, there is a major difference in the hydrodynamic behavior of the two phases: while the solution for the liquid velocity profile needs to be exact to take into account velocity differences near the interface and the wall (in upward inclination the velocity near the pipe wall can be negative), the gas flow can be approximated realistically by full pipe flow. Therefore, the gas side can be treated as bulk flow and the shear stresses are calculated using empirical correlations based on the average velocity. Such an approach simplifies considerably the solution and is capable of taking into account the effective interfacial shear generated by the wavy interface. Note also that the above approach is restricted to low pressure where the density of the gas is small compared to the density of the liquid.

Liquid-Phase Solution

The governing equation for the liquid region is given by Eq. 7. Transforming the liquid boundary conditions into the ξ, η plane yields:

- 1) At $\xi = \pi + \gamma$, $u'_L = 0$ (no slip condition at pipe wall)
- 2) At $\xi = \pi$, $\frac{\partial u'_L}{\partial \xi} = -\frac{\tau_i}{\mu'_{eL}} \frac{c'}{1 + \cosh \eta}$ (interfacial shear stress)
- 3) At $\eta = 0$, $\frac{\partial u'_L}{\partial \eta} = 0$ (symmetry)
- 4) At $\eta \rightarrow \infty$, $u'_L = 0$ (no slip condition at wall interface junction).

The liquid flow rate is calculated by integrating the velocity over the liquid cross-section. Transformation into bipolar coordinates yields

$$\begin{aligned} W'_L &= \frac{W_L}{\rho_L u_{LS} D^2} = 2 \int_0^\infty \int_\pi^{\pi+\gamma} u'_{Lj} d\xi d\eta \\ &= 2c'^2 \int_0^\infty \int_\pi^{\pi+\gamma} \frac{u'_L d\xi d\eta}{(\cosh \eta - \cos \xi)^2} \quad (8) \end{aligned}$$

Note that the dimensionless input flow rate W'_{LI} is $W'_{LI} = \pi/4$.

Gas-Phase Solution

In the gas-phase region a uniform flow in a closed duct is assumed, bounded by the pipe wall and the interface. Wall shear stress and pressure drop are calculated using correlations based on the hydraulic diameter. Following Govier and Aziz (1972), the flow geometrical relations shown in Figure 1 are:

$$\begin{aligned} \gamma &= \cos^{-1}(1 - 2h'_L) \\ A_L &= 0.25 D^2 (\gamma - \sin \gamma \cos \gamma) \\ A_G &= 0.25 D^2 (\pi - \gamma + \sin \gamma \cos \gamma) \\ E_L &= A_L/A \quad E_G = A_G/A \\ S_i &= D\gamma \quad S_G = (\pi - \gamma)D \quad S_i = D \sin \gamma \\ D_L &= \frac{4A_L}{S_L} \quad D_G = \frac{4A_G}{S_G + S_L} \end{aligned} \quad (9)$$

Single-phase correlation based on the hydraulic diameter is used to calculate the shear stress

$$\begin{aligned} \tau_{WG} &= f_G \frac{\rho_G u_G^2}{2} \\ f_G &= C_G (Re_G)^{-m} \end{aligned} \quad (11)$$

The values used for C_G and m in this study are $C_G = 0.046$, $m = 0.2$ for turbulent flow, and $C_G = 16$, $m = 1$ for laminar flow.

An overall force balance on the gas phase yields

$$-A_G \frac{dp}{dz} - \tau_{WG} S_G - \tau_i S_i - \rho_G A_G g \sin \alpha = 0 \quad (12)$$

Measurements of interfacial shear stress for air-water stratified flow were reported by Cohen and Hanratty (1968) for three-dimensional small amplitude waves. Their data were correlated by

$$\lambda_o = 8(u^*/\bar{u}_B)^2 \quad (13)$$

where u^* is the frictional velocity and \bar{u}_B is the average gas velocity taken over the space between the interface and the location of the maximum in the velocity profile of the gas phase. λ_o was found to be constant, which means that small waves behave as a fully developed rough surface. Typically, $\lambda_o = 0.057$ for their data. Using this value for λ_o and assuming $\bar{u}_B = \bar{u}_G = Q_G/A_G$, the interfacial shear stress becomes

$$\tau_i = 0.0142 \frac{\rho_G u_G^2}{2} \quad (14)$$

Cheremisinoff and Davis (1979) used

$$f_i = 0.008 + 2 Re_L \times 10^{-5} \quad (15)$$

for calculating the interfacial shear at the interface. This correlation was first suggested by Miya, Woodmansee and Hanratty for flow between parallel plates up to Reynolds number of 1700. For the range of Reynolds numbers used in this analysis f_i as given by Eq. 15 seems to be unrealistically very high, and therefore was not used here.

The pressure drop, as calculated from the gas phase in dimensionless form is therefore

$$\frac{dP'}{dz'} = \left(-\tau_{WG} \frac{S_G}{A_G} - \tau_i \frac{S_i}{A_G} - \rho_{CG} \sin \alpha \right) \frac{D}{\rho_L u_{LS}^2} \quad (16)$$

This expression for dP'/dz' is used in Eq. 7 to calculate the velocity profile in the liquid phase.

Turbulent Viscosity

Solution of the hydrodynamics of turbulent flow is a problem which cannot be treated rigorously. One of the most acceptable engineering approach for a solution of turbulent flow is to use the concept of the eddy viscosity, which views the Reynolds stresses as an effective turbulent viscosity. The Prandtl mixing length theory has been found very useful for this purpose. According to this theory

$$\mu_t = \rho l_m^2 \left| \frac{du}{dr} \right| \quad (17)$$

Thus, once the mixing length l_m is given the solution of the turbulent flow can proceed. Unfortunately, the determination of the mixing length is not at all straightforward and various correlations have been suggested, usually restricted to a certain region of the flow, based on the distance from the wall.

The most common correlations for the mixing length and the eddy viscosity calculations in pipe flow are given in "wall coordinates" based on the frictional velocity $u^* = \sqrt{\tau_w/\rho}$, which defines the dimensionless distance $y^+ = yu^*/\nu$. Launder and Spalding (1972) have summarized many such correlations. Some of the most widely used are:

1) Deissler's equation for the region near the wall ($0 \leq y^+ \leq 20$)

$$\epsilon_t = \mu_t/\rho = 0.01 u y [1 - \exp(-0.01 u y/\nu)] \quad (18)$$

2) Von Karman equation for the turbulent core ($y^+ > 20$)

$$\epsilon_t = \mu_t/\rho = 0.362 \frac{(du/dr)^3}{(d^2u/dr^2)^2} \quad (19)$$

3) Van Driest model for the entire flow cross-section

$$l_m = ky[1 - \exp(-y^+/26)] \quad k = 0.4 \quad (20)$$

The aforementioned correlations are strictly for full pipe flow. Extension to stratified flow needs further elaboration. The correlations are given in terms of the radius r or the radial distance from the wall y . For stratified flow in partially filled pipe the use of the distance along the radial direction is not appropriate because the flow field is two-dimensional. Furthermore, for $h_L/D > 0.5$, this distance is meaningless for the region above the pipe centerline. Thus it is suggested to measure y along the line $\eta = \text{const}$. Note that near the wall the η lines coincide with the y (or r) lines.

Another difficulty arises in applying the eddy viscosity correlation for pipe flow (Eqs. 19 and 20) to the turbulent "core" of stratified flow, namely to the region near the interface. Strict application of Eq. 20 in this case will result very high values of the eddy viscosity as a result of the large velocity gradients obtained at the interface. This is in contradiction to the values of the eddy viscosity obtained in similar geometries. Shlichting (1960) shows that the eddy viscosity decreases close to the pipe center line. For a similar geometry of closed channel flow Quarmby and Quirk (1972) and Hussain and Reynolds (1975) showed the eddy viscosity approaches approximately a constant value near the center. Experiments in open channel flow (Ueda et al., 1977) showed that the eddy viscosity decreases near the interface. From the aforementioned it is clear that the high values obtained for the eddy viscosity in this case (owing to the large velocity gradient) is not physical and the eddy viscosity probably is either constant or decreases close to the interface.

In this work a tentative suggestion is made to use the Van Driest model near the wall and to apply a constant value in the turbulent core. Van Driest model is assumed to be valid up to $y^+ = 30$ and for $y^+ > 30$ a constant value, which has the value as that at $y^+ = 30$ is used. Admittedly the choice of $y^+ = 30$ is somewhat arbitrary. For full pipe flow this method would give reasonable results at low Reynolds number and it is quite possible that our results here are limited to Reynolds number below 10,000. Note that for stratified flow to exist the flow rates should be low and the Reynolds number is usually below 10,000. One has also to realize that the variation of the eddy viscosity in this case is unknown and is a subject of a separate study. The procedure of solution could be modified latter to accommodate more recent information. At any rate our assumption will be tested against data for pressure drop and agreement with experiment is an indication that this procedure is sufficiently accurate at least for the prediction of the pressure drop.

Note also that for evaluating y^+ , the wall shear is based on the average absolute value of τ_{WL} .

The Van Driest model, as modified for our case, will therefore read

$$l'_m = kl'_\xi [1 - \exp(-l_\xi^+/26)] \quad (21)$$

$$\mu'_{tL} = l_m'^2 \left| \frac{\partial u_L}{\partial \xi} \right| = l_m'^2 \left| \frac{\partial u_L}{\partial \xi} \frac{\cosh \eta - \cos \xi}{c'} \right| \quad (22)$$

where l_ξ is the distance from the pipe wall as measured along the $\eta = \text{const}$. lines, and $l_\xi^+ = (l_\xi D \sqrt{\tau_{WL}/\rho_L})/\nu_L$. The average shear

stress at the pipe wall, τ_{WL} , can be calculated by an overall momentum balance on the liquid phase.

$$\tau_{WL} = \tau_t \frac{S_i}{S_L} - \rho_L g \sin \alpha \frac{A_L}{S_L} - \frac{dP}{dz} \frac{A_L}{S_L} \quad (23)$$

An arc length element along the line $\eta = \text{const}$.

$$dl'_\xi = \frac{c'}{\cosh \eta - \cos \xi} d\xi \quad (24)$$

Integrating dl'_ξ from ξ to $\xi = \pi + \gamma$ results in

$$l'_\xi = \int_\xi^{\pi+\gamma} \frac{c'}{\cosh \eta - \cos \xi} d\xi \quad (24')$$

Along the lines $\eta = \text{const}$ $\cosh \eta = \text{const} = B \geq 1$, thus

$$l'_\xi = \frac{2c'}{\sqrt{B^2 - 1}} \left[\tan^{-1} \left(\sqrt{\frac{B+1}{B-1}} \tan \frac{\pi + \gamma}{2} \right) - \tan^{-1} \left(\sqrt{\frac{B+1}{B-1}} \tan \frac{\xi}{2} \right) \right] \quad (25)$$

Equation 25 permits the calculation of the distance of any point (ξ, η) from the pipe wall along the η lines. Note, however, that for the points along the interface where $\xi = \pi$

$$\lim_{\xi \rightarrow \pi+\epsilon} \tan^{-1} \left(\sqrt{\frac{B+1}{B-1}} \tan \frac{\pi}{2} \right) \rightarrow -\frac{\pi}{2} \quad (25')$$

Numerical Solution

The momentum equation for the liquid phase, as given by Eq. 7, with the boundary conditions, is solved numerically using a finite difference technique. Due to symmetry with respect to the vertical diameter, the solution is carried out on half the pipe cross-section. The region of solution is unbounded in the η direction. In practice the upper limit of η is taken as a finite large number. Taking $\eta = 10$, for example, replaces the pipe wall-interface junction point by a circular arc with a radius of $10^{-5} \times R$. At this region the velocity approaches zero and the error introduced by truncating η is minimal. In order to avoid a large number of grid points in the η direction a variable increasing increment step is used. The increment step in the ξ direction is also variable: A finer grid must be used near the pipe wall and the interface where the velocity gradients in the ξ direction changes substantially.

Expanding $u'_{L(i,j)}$ in Taylor's series and solving for the first and second partial derivatives, Eq. 7 can be converted into a discrete form. (For brevity $u_{i,j}$ is used instead of $u'_{L(i,j)}$):

$$\begin{aligned} & \frac{(u_{i,j+1} - u_{i,j})\Delta\xi_j - (u_{i,j} - u_{i,j-1})\Delta\xi_{j+1}}{\xi_d/2} \\ & + \frac{(u_{i+1,j} - u_{i,j})\Delta\eta_i - (u_{i,j} - u_{i-1,j})\Delta\eta_{i+1}}{\eta_d/2} \\ & = \frac{K'_L}{\mu'_{eL(i,j)}} \frac{c'^2}{(\cosh \eta_i - \cos \xi_j)^2} \end{aligned} \quad (26)$$

where

$$\begin{aligned} \eta_d &= \Delta\eta_i \quad \Delta\eta_{i+1} \quad (\Delta\eta_i + \Delta\eta_{i+1}) \\ \xi_d &= \Delta\xi_j \quad \Delta\xi_{j+1} \quad (\Delta\xi_j + \Delta\xi_{j+1}) \\ \mu'_{eL(i,j)} &= \frac{1}{R_{eLS}} + l_m'^2 \left| \frac{\partial u_L}{\partial \xi} \right| \left| \frac{(u_{i,j+1} - u_{i,j})\Delta\xi_j^2 - (u_{i,j-1} - u_{i,j})\Delta\xi_{j+1}^2}{\xi_d} \right. \\ & \quad \times \frac{\cosh \eta_i - \cos \xi_j}{c'} \end{aligned}$$

Solving for $u_{i,j}$:

$$u_{i,j} = P_1 u_{i,j-1} + P_2 u_{i+1,j} + P_3 u_{i,j+1} + P_4 u_{i-1,j} - P_5 \quad (27)$$

where

$$\begin{aligned} P_d &= \eta_d (\Delta\xi_j + \Delta\xi_{j+1}) + \xi_d (\Delta\eta_i + \Delta\eta_{i+1}) \\ P_1 &= \frac{\Delta\xi_{j+1} \eta_d}{P_d} \end{aligned}$$

$$P_2 = \frac{\Delta \eta_i \xi_d}{P_d}$$

$$P_3 = \frac{\Delta \xi_j \eta_d}{P_d}$$

$$P_4 = \frac{\Delta \eta_{i+1} \xi_d}{P_d}$$

$$P_5 = \frac{\frac{K'_L \xi_d \eta_d}{2P_d} \frac{c'^2}{(\cosh \eta_i - \cos \xi_j)^2}}{\mu_{eL(i,j)}}$$

Equation 27 is solved iteratively in order to calculate interior grid point velocities.

Along the boundary $\eta = 0$, the first derivative with respect to η is set to zero, using the mirror image approach, i.e., applying Eq. 27 with $u_{i-1,j} = u_{i+1,j}$.

At the interface, the first derivative with respect to ξ is

$$u_{i,1} = \Delta \xi_1 \frac{\tau' c'}{\mu_{eL(i,1)}(1 + \cosh \eta_i)} + u_{i,2} \quad (28)$$

Method of Solution.

The solution is carried out iteratively along the following steps.

1. Physical properties and operational conditions are set. This includes the liquid and gas flow rates u_{LS} and u_{GS} .

2. A value for h_L/D is assumed and all the geometrical variables which depend on h_L/D are calculated (Eq. 9). Note that the first guess for h_L/D is taken from Taitel and Dukler (1976).

3. The pressure drop is calculated using the appropriate correlations for the gas bulk flow (Eq. 16).

4. The average wall shear stress τ_{WL} is calculated using Eq. 23. Likewise the mixing length l_m at each grid point is determined.

5. The velocity profile of the liquid phase is calculated using the Gauss-Seidel iterative technique (Eqs. 27 and 28).

6. The liquid flow rate is calculated by Eq. 8 and compared with the input flow rate ($\pi/4$). Steps 2 and 6 are repeated until convergence of the flow rate is achieved.

RESULTS

The results of the present theory reported here are for air-water systems in a 25.4 mm pipe at 25°C and 1 atm.

Typical results of the velocity field over half the liquid phase cross section are shown in Figures 3, 4 and 5 for horizontal, upward inclined and downward inclined flow, respectively. The abscissa is the distance from the normal midplane and the ordinate the distance from the bottom pipe wall. The velocity is normalized with respect to the maximum velocity, namely $u'_L/u'_{L(max)}$, where $0 \leq |u'_L/u'_{L(max)}| \leq 1$. In all these three examples the flow rates are $u_{LS} = 0.1$ m/s and $u_{GS} = 1$ m/s.

Figure 3 shows the velocity field for the horizontal configuration. As can be observed, the velocity depends mostly on the radial coordinate, varying from zero on the pipe wall to the maximum velocity near the pipe center. In such a case the velocity can be approximated by $u = u(r)$ as assumed by Cheremisinoff and Davis (1979).

Figure 4 represents the velocity field for a 10° upward inclined flow. The velocity field in this configuration is completely different from that of the horizontal case. The upper liquid layer moves at a higher velocity in the flow direction due to the shear exerted by the gas phase at the interface. However, near the lower pipe wall the liquid flows backwards resulting in a negative shear on the pipe surface. In this region curves of constant velocity are closed contours. The zero velocity line intersects the pipe wall separating the flow cross-section into forward and backward flows. Clearly the one-dimensional approach, which is based on the calculation of the shear stress on the average velocity, does not apply here (as it yields a positive shear).

In downward inclined flow, Figure 5, all the liquid moves forward in the flow direction, with a considerably lower equilibrium

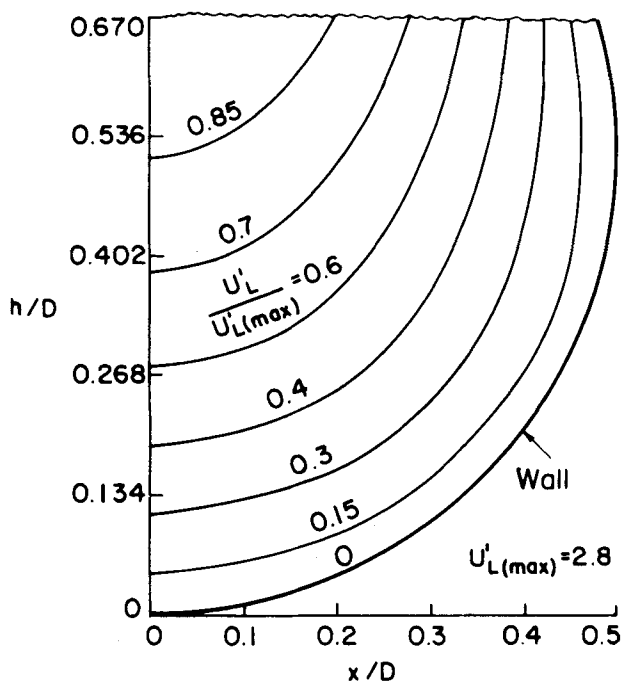


Figure 3. Velocity field for horizontal flow

($u_{LS} = 0.1$ m/s, $u_{GS} = 1$ m/s).

liquid level as compared to the horizontal flow. The velocity field is, however, similar to that of the horizontal case, as it is always in the positive direction.

Experimental data for holdup and pressure drop in stratified flow are available in the literature for horizontal flow only. Such data are found in the works of Berglin (1949), Hoogendoorn (1959), Govier (1962), Agrawal (1973), and Cheremisinoff and Davis

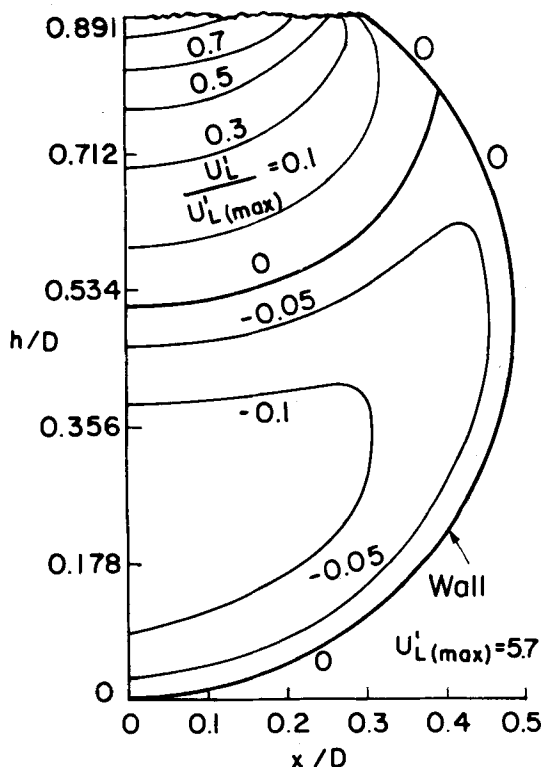


Figure 4. Velocity field for upward inclined flow

($\alpha = 10^\circ$, $u_{LS} = 0.1$ m/s, $u_{GS} = 1$ m/s).

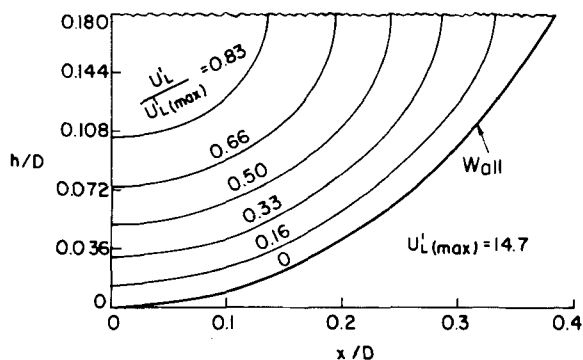


Figure 5. Velocity field for downward inclined flow

($\alpha = -10^\circ$, $u_{LS} = 0.1$ m/s, $u_{GS} = 1$ m/s).

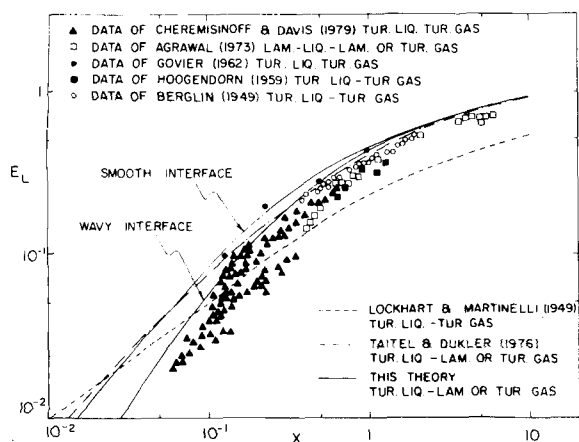


Figure 6. Holdup: comparison between theory and experimental data.

(1979). The data are usually presented in the form of E_L and ϕ_G vs. X , where E_L is the liquid holdup,

$$\phi_G^2 = \left| \left(\frac{dP}{dz} \right)_{TP} \right| / \left| \left(\frac{dP}{dz} \right)_{GS} \right|$$

is the ratio of the two phase to the single gas-phase pressure drop and X is the Lockhart and Martinelli parameter.

Turbulent stratified flow in air-water systems in horizontal pipes takes place over quite a narrow range of liquid flow rates, namely $0.08 \text{ m/s} < u_{LS} < 0.12 \text{ m/s}$. Thus the value of $u_{LS} = 0.1 \text{ m/s}$ was chosen to represent the results of the present theory for horizontal flow.

Figures 6 and 7 show the comparison between holdup and pressure drop predicted by the present analysis and the experimental measurements obtained by the aforementioned investigators. Also shown in the figures are the correlation of Lockhart and Martinelli (1949) and the Taitel and Dukler (1976) one-dimensional model. The results of the present theory are plotted for two cases of shear: the first correlation assumes smooth interface conditions, while the second correlation is for small amplitude waves (Eq. 14).

As shown in Figure 6 the results of our analysis for the liquid holdup under smooth interface conditions and the results of the Taitel and Dukler model are very close. For wavy interfacial structure, however, the present analysis predicts lower values for E_L than the Taitel and Dukler model for $X < 0.1$ and shows better agreement with the experimental measurements. Small values of X represent high gas and low liquid flow rates, where waves develop on the interface. Under these conditions the present theory naturally agrees better with the experimental data, since it takes into account the interfacial structure. Most of the data, particularly for low values of X , indicate that the prediction of Eq. 14 for the

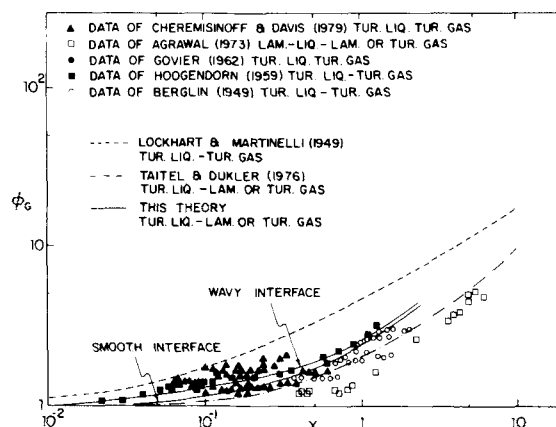


Figure 7. Two-phase pressure drop: comparison between theory and experimental data.

shear stress is probably somewhat lower, especially for the case where roll waves develop (at about $X \approx 0.1$). Unfortunately, a satisfactory correlation for the shear stress for roll waves has not been found. However, it is clear that such a correlation will yield lower values of E_L that would agree better with experiment. This is, however, outside the scope of the present work.

A similar comparison of the dimensionless pressure drop ϕ_G is given in Figure 7. As can be seen, the Lockhart and Martinelli correlation predicts considerably higher values of ϕ_G as compared to the experimental data. The Taitel and Dukler model, on the other hand, forms a lower bound for the turbulent data points. As expected, the prediction of this analysis for a wavy interface is higher than for a smooth interface condition, and agrees somewhat better with the experimental data. This data points above the curve for the wavy interface correspond to the development of roll waves on the interface. As aforementioned, these data points can be predicted by the present theory provided that a suitable correlation for the interfacial shear stress under a roll waves condition is available.

The effect of the pipe inclination of the liquid equilibrium level and pressure drop is demonstrated in Figures 8, 9 and 10. In these figures the solution for a smooth interface is used and a comparison with the Taitel and Dukler model is made. The liquid flow rate varies between 0.05 to 1 m/s. In the lower range the flow is usually not yet turbulent, while in the upper range the flow is no longer stratified in the horizontal and upward flows. Though the range of liquid flow rates covered exceeds the range of the actual turbulent stratified flow conditions, it does however clearly demonstrate the effect of the liquid flow rate. The gas flow rate varies between 0.01 to 100 m/s covering laminar and turbulent flows.

As expected, the equilibrium liquid depth is considerably greater in upward inclined flow as compared to horizontal flow, whereas in downward inclined flow the liquid level is considerably lower than that for horizontal flow under the same conditions. As an example, for the flow rates of $u_{LS} = 0.1 \text{ m/s}$ and $u_{GS} = 1 \text{ m/s}$, the liquid level h_L/D is 0.66, 0.89 and 0.18 for horizontal, upward inclined ($+10^\circ$) and downward inclined (-10°) flows, respectively. In upward inclined flow gravity forces are opposite to the flow direction, resulting in a lower liquid velocity and higher liquid level in the pipe. In downward inclined flow, on the other hand, the velocity is much higher and the liquid level in the pipe is lower.

The same trends are basically observed in the figures for the pressure drop. Comparing ϕ_G for the same flow conditions, it is again observed, as expected, that the pressure drop in upward inclined flow is much higher than in horizontal flow and considerably lower in downward inclined flow.

Generalization of Results

The solution of Eq. 7 with the proper boundary conditions and the turbulent viscosity evaluated by Eq. 22 shows that the equi-

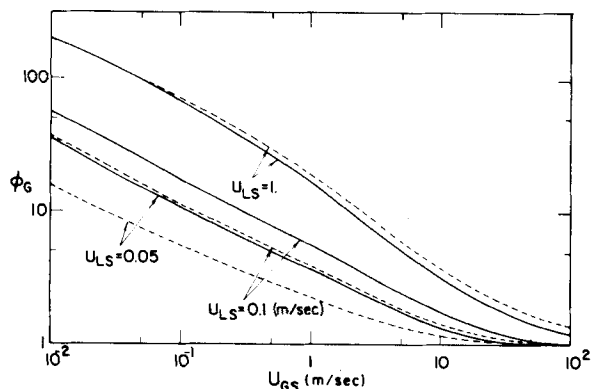
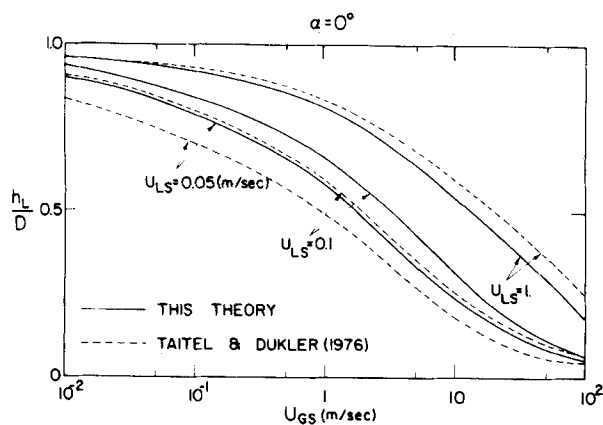


Figure 8. Holdup and pressure drop for air water systems (horizontal flow).

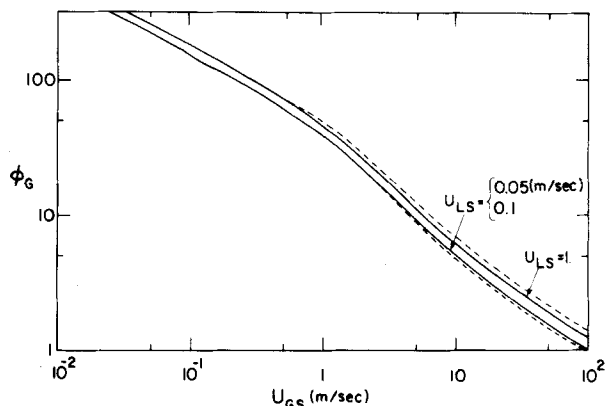
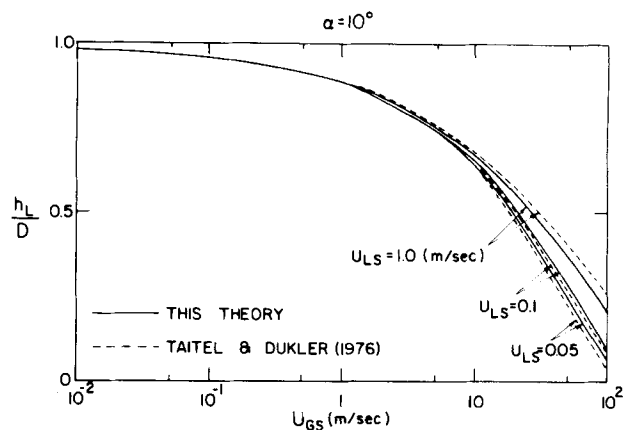


Figure 9. Holdup and pressure drop for air water systems (10° upward inclination).

librium liquid level in stratified turbulent flow depends on the following dimensionless groups:

$$\frac{h_L}{D} = f(K'_L, Re_{LS}, \tau'_i, Re^*) \quad (29)$$

where

$$\begin{aligned} K'_L &= \left\{ \frac{dP}{dz} + \rho_L g \sin \alpha \right\} \frac{D}{\rho_L u_{LS}^2} \\ Re_{LS} &= \frac{u_{LS} D}{\nu_L} \\ \tau'_i &= \frac{\tau_i}{\rho_L u_{LS}^2} \\ Re^* &= \frac{D \sqrt{|\tau_{WL}|}}{\nu_L} \end{aligned} \quad (30)$$

The average liquid wall shear stress τ_{WL} is calculated from an overall momentum balance on the liquid phase (Eq. 23). Converting this equation into dimensionless form yields

$$A'_L K'_L - \left(\frac{Re^*}{Re_{LS}} \right) S'_L + \tau'_i S'_i = 0 \quad (31)$$

Note that Re^* can be expressed by the other groups and eliminated from Eq. 29. Thus the solution depends on

$$\frac{h_L}{D} = f(K'_L, Re_{LS}, \tau'_i) \quad (32)$$

It is suggested, however, to present the results in the form

$$\frac{h_L}{D} = f(K'_L, Re_{LS}, G'_e) \quad (33)$$

where

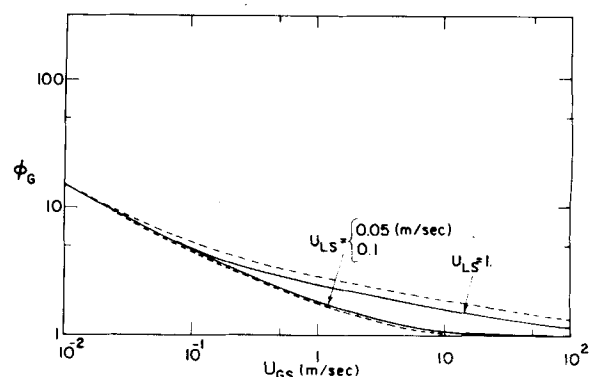
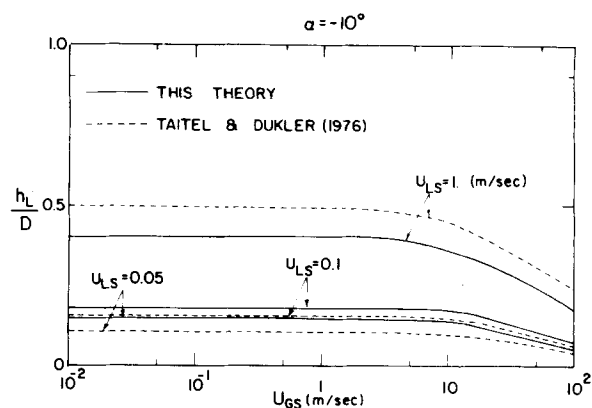


Figure 10. Holdup and pressure drop for air water systems (10° downward inclination).

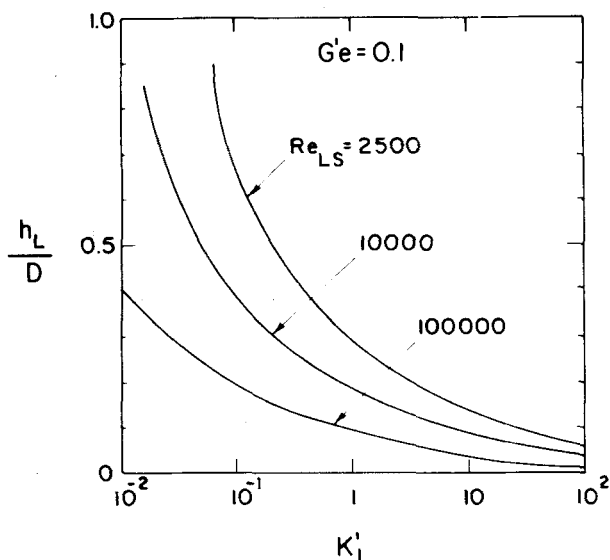


Figure 11. Generalized equilibrium liquid level for $Ge' = 0.1$.

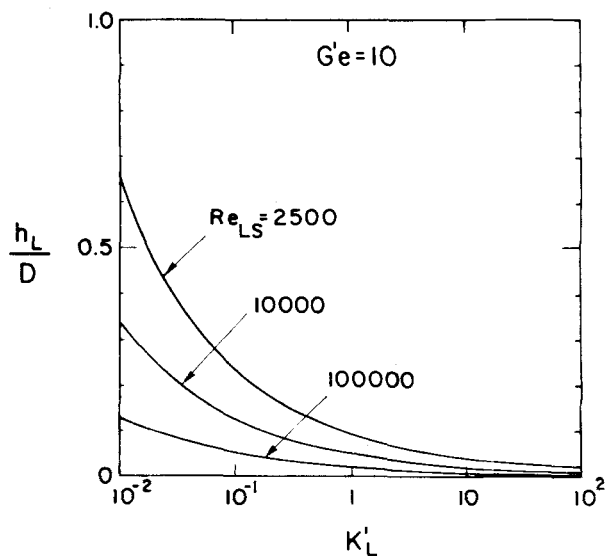


Figure 13. Generalized equilibrium liquid level for $Ge' = 10$.

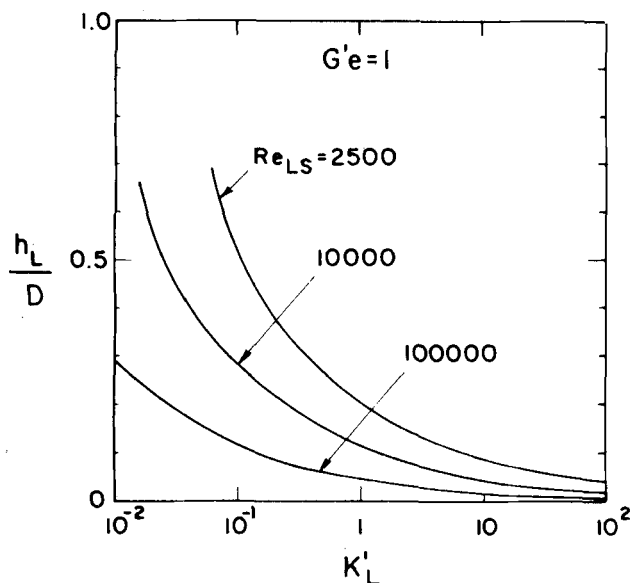


Figure 12. Generalized equilibrium liquid level for $Ge' = 1$.

$$G'_e = \frac{4\tau'_i}{K'_L} \frac{4\tau_i/D}{\left\{ \frac{dP}{dz} + \rho_L g \sin \alpha \right\}} \quad (34)$$

since G'_e is not sensitive to the liquid and gas flow rates (contrary to τ'_i). In horizontal flow

$$G'_e = \frac{\frac{4}{D} f_i \frac{\rho_G u_G}{2}}{\frac{4}{D} f_G \frac{\rho_G u_G^2}{2}} = \frac{D_G f_i}{D f_G} \quad (35)$$

thus for smooth interface conditions where $f_i/f_G \rightarrow 1$, the solution depends only on

$$\frac{h_L}{D} = f(K'_L, Re_{LS}) \quad (36)$$

The result of Eq. 36 is also obtained for $f_i/f_G \approx \text{constant}$

Equation 36 shows that h_L/D depends on two parameters K'_L and Re_{LS} . This relation is equivalent also to the relation

$$\frac{h_L}{D} = f(X, Re_{LS}) \quad (37)$$

namely that the liquid equilibrium level, or the holdup, depends on the Lockhart and Martinelli parameter and the superficial Reynolds number. Note, however, that Eq. 37 is different for different values of f_i/f_G .

Figure 6 shows the experimental results in the form of $h_L/D = f(X, Re_{LS}, f_i/f_G)$. As explained above, this is indeed a valid single representation for the holdup.

Likewise, it can be shown that ϕ_G , the dimensionless pressure drop is only a function h_L/D and f_i/f_G , and thus can be represented as a function of the same variables. This is shown in Figure 7.

A generalized solution of Eq. 33 that covers a range which can be of practical importance is given in Figures 11, 12 and 13 for $G'_e = 0.1, 1$ and 10 . These figures can be used to obtain a solution using the following procedure:

1. Assume value for h_L/D .
2. Calculate K'_L , Re_{LS} and G'_e from Eqs. 30 and 34 using Eqs. 16 and 14 to determine the pressure drop and the interfacial shear stress.
3. Find a new value for h_L/D using Figures 11 to 13.
4. Repeat steps 2 and 3 with the new value of h_L/D until convergence is reached.

NOTATION

A	= area, m^2
B	= constant
C	= constant
c	= half the interface length, m
D	= diameter, m
E	= void fraction
f	= friction factor
f'	= dimensionless group (Eq. 34)
g	= acceleration of gravity, m/s^2
h	= liquid level, m
i	= index along η , also $\sqrt{-1}$
Ja	= Jacobian
j	= index along ξ
K'_L	= dimensionless group
l	= length, m
m	= exponent
P	= pressure, N/m^2
P_1, P_2, \dots	= coefficients (Eq. 27)

Q	= volumetric flow rate, m^3/s
R	= radius, m
r	= radial coordinate
Re	= Reynolds number
Re^*	= dimensionless group
S	= perimeter, m
u	= velocity, m/s
u^*	= friction velocity ($\sqrt{\tau_w/\rho}$), m/s
W	= mass flow rate, kg/s
X	= Lockhart and Martinelli parameter = $[(dP/dx)_{LS}/(dP/dx)_{GS}]^{1/2}$
x	= cartesian coordinate
y	= cartesian coordinate
y^+	= dimensionless distance (yu^*/ν)
z	= coordinate in the flow direction

Greek Letters

α	= angle of inclination
γ	= angle defined by the interface
ϵ_t	= eddy viscosity, m^2/s
η	= bipolar coordinate
λ_o	= friction factor defined by Eq. 13
μ	= viscosity, $kg/m \cdot s$
ν	= kinematic viscosity, m^2/s
ξ	= bipolar coordinates
ρ	= density, kg/m^3
τ	= shear stress, N/m^2
τ_i	= dimensionless shear group ($\tau_i/\rho_L u_{LS}^2$)
ϕ	= Lockhart and Martinelli pressure drop parameter $[(dp/dx)/(dp/dx)_{GS}]^{1/2}$

Subscripts

e	= effective
G	= gas
i	= interface
L	= liquid
m	= mixing
S	= superficial
TP	= two phase
t	= turbulent
W	= wall

LITERATURE CITED

- Agrawal, S. S., G. A. Gregory, and G. W. Govier, "An Analysis of Horizontal Stratified Two Phase Flow in Pipes," *Can. J. Chem. Eng.*, **51**, p. 280 (1973).
- Bergelin, O. P., and C. Gazley, "Cocurrent Gas Liquid Flow in Horizontal Tubes," *Proc. Heat Tran. and Fluid Mech. Inst.*, **29**, p. 5 (1949).
- Cheremisinoff, N. P., and E. J. Davis, "Stratified Turbulent-Turbulent Gas-Liquid Flow," *AIChE J.*, **25**, p. 48 (1979).
- Cohen, S. L., and T. J. Hanratty, "Effects of Waves at a Gas-Liquid Interface on a Turbulent Air Flow," *J. Fluid Mech.*, **31**, p. 467 (1968).
- Dukler, A. E., "Fluid Mechanics and Heat Transfer in Vertical Falling Film Systems," *Chem. Eng. Prog. Sym. Ser.*, **56** (1960).
- Etchells, A. W., "Stratified Horizontal Two-Phase Flow in Pipes," Ph.D. Thesis, University of Delaware (1970).
- Govier, G. W., and K. Aziz, *The Flow of Complex Mixtures in Pipes*, Van Nostrand Reinhold Co. (1972).
- Govier, G. W., and M. M. Omer, "The Horizontal Pipeline Flow of Air-Water Mixtures," *Can. J. Chem. Eng.*, **40**, p. 93 (1962).
- Hoogendoorn, C. L., "Gas Liquid Flow in Horizontal Pipes," *Chem. Eng. Sci.*, **9**, p. 205 (1959).
- Hussain, A. K. M. F., and W. C. Reynolds, "Measurements in Fully Developed Turbulent Channel Flow," *J. of Fluids Eng.*, ASME, p. 568 (Dec., 1975).
- Johannessen, T., "A Theoretical Solution of the Lockhart and Martinelli Flow Model for Calculating Two Phase Flow Pressure Drop and Holdup," *Int. J. Heat Mass Transfer*, **15**, p. 1443 (1972).
- Kadambi, J., "Void Fraction and Pressure Drop in Two Phase Stratified Flow," *Can. J. of Chem. Eng.*, **59**, p. 584 (1981).
- Launder, B. E., and D. B. Spalding, *Mathematical Models of Turbulence*, Academic Press (1972).
- Lockhart, R. W., and R. C. Martinelli, "Proposed Correlation of Data for Isothermal Two Phase, Two Component Flow in Pipes," *Chem. Eng. Prog.*, **45**, p. 38 (1949).
- Quarmby, A., and R. Quirk, "Measurements of the Radial and Tangential Eddy Diffusivities of Heat and Mass in Turbulent Flow in a Plain Tube," *Int. J. Heat Mass Trans.*, **15**, p. 2309 (1972).
- Russell, T. W. F., A. W. Etchells, R. H. Jensen, and J. P. Arruda, "Pressure Drop and Holdup in Stratified Gas-Liquid Flow," *AIChE J.*, **20**, p. 664 (1974).
- Schlichting, H., *Boundary Layer Theory*, 4th Ed., McGraw-Hill (1960).
- Taitel, Y., and A. E. Dukler, "A model for Predicting Flow Regime Transition in Horizontal and Near Horizontal Gas Liquid Flow," *AIChE J.*, **22**, p. 47 (1976).
- Ueda, H., R. Moller, S. Komori, and T. Mizushima, "Eddy Diffusivity Near the Free Surface of Open Channel Flow," *Int. J. Heat Mass Tran.*, **20**, p. 1127 (1977).

Manuscript received August 10, 1982; revision received May 17, and accepted May 31, 1983.